ORIGINAL ARTICLE

Assessing hydrochemical evolution of groundwater in limestone terrain via principal component analysis

Zargham Mohammadi

Abstract This paper describes the use of multivariate statistical analysis to trace hydrochemical evolution in a limestone terrain at Zagros region, Iran. The study area includes a deep confined aquifer, overlaid by an unconfined aquifer. The method involves the use of principal component analysis (PCA) to assess and evaluate the hydrochemical evolution based on chemical and isotope variables of 12 piezometers drilled in both the unconfined and confined aquifers. First PCA on all variables shows that water–rock interaction under different conditions with respect to the atmospheric CO_2 is the main process responsible for chemical constituents. As a result, combinations of several ratios such as Ca/TDS, SO_4/TDS and Mg/TDS with physico-chemical and isotope variables reveal different hydrochemical evolution trend in the aquifers. Second PCA on the selective samples and variables reveals that displacement of the unconfined samples from dry to wet season follows a refreshing trend towards river samples that is characterized by reducing electrical conductivity and increasing sulphate and tritium contents. However, the refreshing trend cannot be traced in the confined aquifer samples suggesting no recharge from river to the confined aquifer. Third PCA reveals that, chemical composition of water samples in the unconfined aquifer tends to have considerable difference from each other in the end of recharge period. In contrast, the confined aquifer samples have a tendency to show similar chemical composition during recharge period in comparison to end of dry period. This difference is caused by different mechanism of recharge in the unconfined aquifer (through the whole aquifer surface) and the confined aquifer (through the limited recharge area).

Introduction

Limestone aquifers are suitable resources, sometimes the only ones available for drinking and agriculture in many parts of the world. It is estimated that 25% of the world's population, including many large cities and extensive rural areas, depends on karst water supplies to sustain their daily activities (Ford and Williams 1989). The total area of carbonate rock outcrops in Iran is about 185,000 km^2 (11% of Iran's land area), 55.2% of which extend to the Zagros region, south and south-west of Iran (Raeisi and Kowsar 1997).

Limestone aquifers have an extensive heterogeneity if they are karstified. Groundwater system in such aquifers is difficult to understand and needs a systematic methodology including delineation of karst structure, karst functioning by means of artificial and natural tracers and modelling approach (Bakalowicz 2005; Mohammadi 2006). Natural tracing by using the chemical composition of groundwater (e.g. groundwater geochemistry) has contributed significantly to the understanding of groundwater system over the last 50 years (Glynn and Plummer 2005). In general, the chemical composition of natural water results from three factors: (1) the type of rock in contact with the flowing water, (2) the environmental conditions, e.g. temperature and pressure, and (3) the flow conditions, e.g. water velocity (Bakalowicz 1994). These factors combine to create diverse water types that change spatially and

Z. Mohammadi (✉)
Department of Earth Science, College of Science,
Shiraz University, 71454 Shiraz, Iran
e-mail: zmohamad@shirazu.ac.ir

temporally. The measurement of naturally occurring parameters is an integral part of water resource assessment and management. Among them, the use of major ions has become a very common method to divide the samples into hydrochemical facies that can be correlated with location and/or flow system. Sampling for hydrochemical analysis, e.g. major ions and stable isotopes is suggested to be carried out from wells and springs at the same time, at different seasons.

In order to facilitate the classification of samples, several commonly used graphical methods and multivariate statistical techniques are available (Guler et al. 2002) including Collins bar diagram, pie diagram, stiff pattern diagram, Schoeller semi-logarithmic cluster analysis, Piper diagram, Q-mode hierarchical cluster analysis, K-means clustering, principal component analysis, and fuzzy-k-mean clustering. The principal component analysis (PCA) of physico-chemical data is widely used to characterize and evaluate surface and groundwater quality, and it is useful for evidencing temporal and spatial variation caused by natural and human factors linked to seasonality (Bakalowicz 1994; Helena et al. 2000; Andreo et al. 2002; Karimi et al. 2005). PCA reduces the dimensionality of a highly dimensioned data set by explaining the correlation among a large number of variables in terms of smaller number of underlying factors (i.e. principal components or PCs).

The present study attempts to clarify the main controlling factors of chemical composition and chemical evolution. The study area is located in the Zagros region, southern Iran (Fig. 1). The investigated area has been described in previous works (e.g. Mahab Ghods Consulting Engineers 2000; Karimi 2003; Mohammadi et al. 2007a). The existence of two different aquifers including unconfined and confined in the study area is also addressed. The structure of the aquifers was delineated and their behaviour was studied by hydrodynamic and hydrochemical time series (Mohammadi et al. 2007a). In this study, chemical relationships between samples from both confined and unconfined aquifers are assessed, and their chemical evolution in each aquifer is investigated using PCA. The objectives of the present study are (1) delineation of the main processes responsible for the concentration of inorganic dissolved compounds, and (2) assessment of the chemical evolution from the low-flow stage to the recharge period in both confined and unconfined aquifers.

Geological framework

The area under study is situated in the Zagros region, southern Iran (Fig. 1). Zagros region is one of five major structural zones in Iran (Stocklin 1968). The stratigraphy and structural framework of the Zagros region have been studied in detail by Stocklin and Setudehnia (1977) and Alavi (2004). The stratigraphy sequence in the study area ranges from Oligocene to Miocene in age consisting of two main formations, the Asmari (Oligocene–Miocene) and Gachsaran (Miocene) formations (Fig. 1). The Asmari formation is characterized by limestone with interbedded marl. It can be divided into lower and upper units: the 250-m-thick lower Asmari (L.AS) is composed of a sequence of thin limestone beds, marly limestone and dolomite; and the 235-m-thick upper Asmari (U.AS) is composed of thick bedded limestone. Overlying the Asmari limestone, the Gachsaran formation (GS) is composed of salt, anhydrite, marl and gypsum. The GS outcrops at limited areas at low elevation on both sides of the Khersan River, upstream from the study area. A thin layer of quaternary alluvium (Qt) is also exposed at the bottom of the main valley (Fig. 1).

Structurally, the study area is formed of Rig and Laki anticlines, separated with the narrow Shosh syncline. These anticlines are mainly formed by Asmari limestone. The Khersan River crosses the Laki Anticline perpendicularly in deep gorges (Fig. 1).

Hydrogeological setting

The regional hydrogeology was described by Mahab Ghods Consulting Engineers (2000), Karimi (2003) and Mohammadi et al. (2007a), based on hydrodynamics, water chemistry and isotope data. The two main aquifers are (1) a confined aquifer in the lower Asmari limestone and (2) an unconfined aquifer in the upper and partly in the lower Asmari limestone (Fig. 2). They are separated by a 5-m-thick marly layer (Fig. 2). However, in a detailed recent study, the confined limestone aquifer system was differentiated into three sub-aquifers (Mohammadi et al. 2007a), according to variation of chemical and isotope content over 1 year. In the present study (Fig. 2), we will consider, a priori, only the two independent aquifers as it was done in the first studies (Mahab Ghods Consulting Engineers 2000; Karimi 2003).

Three types of screened piezometers were installed (Fig. 2): (1) those controlling the unconfined aquifer (U14, U15, U16, U22, U24, U29, U20, U21, U33, U31, and U25), (2) those controlling the confined aquifer (C1, C34, C3, C22, C17, and C19,) and (3) those which are not completely sealed at the confining layer, and consequently allow a mixing of ground water from both aquifers (C2, C4, C6, C8 and C11). They are implemented on both banks of the Khersan River (Fig. 2).
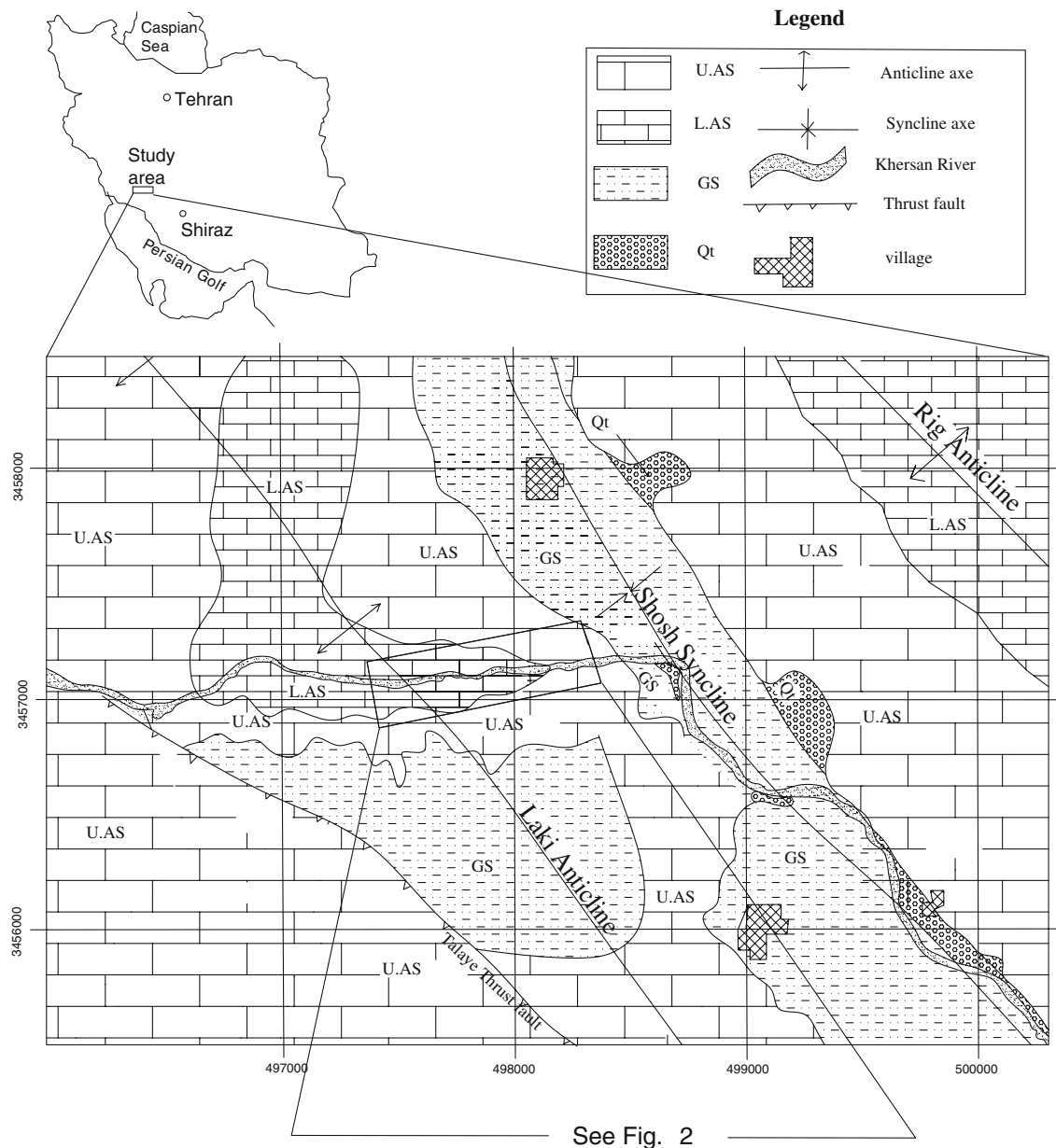
Fig. 1 The study area. Location, geological framework and location of piezometers a presented in Fig. 2

The unconfined aquifer

The water level in the unconfined sub-aquifer ranges from 1,264 to 1,273.2 m above sea level (asl). The water level in the right bank piezometers is 0.8–2 m higher than the Khersan River and 0.57–3.48 m higher than in the left bank piezometers, indicating a general flow direction in the unconfined aquifer from right to left bank (Karimi et al. 2007). The unconfined aquifer is mainly recharged by direct infiltration on Asmari outcrops, and locally through the GS when it overlies limestone; a concentrated recharge also occurs from surface runoff through karstic swallow holes. Most recharge occurs during December–April. Isotope analysis of the groundwater shows that the recharge water to the unconfined aquifer originates mostly from areas about 1,300 to 1,500 m asl (Mohammadi 2006).

Despite the absence of solution cavities in the boreholes and of surface karst features in the study area, the rapid changes of the physico-chemical parameters such as water level and electrical conductivity (EC) in piezometers in response to rain events during the wet season, suggest that karst phenomena probably developed locally and account for the fast ground water flow rather than storage (Karimi et al. 2007). Chemical and isotope natural tracing indicates

that the unconfined aquifer behaviour is related to the existence of solution conduits at local as well as regional scale (Mohammadi et al. 2007a).

The confined aquifer

The piezometric level in the confined aquifer ranges from 1,297 to 1,359 m asl. Minimum and maximum flow rates from artesian wells range from 0.4 to 20 L s^{-1} (Mohammadi et al. 2007a). The lowest pressure was observed to be around 0.2 atm. in C11 and C6 (Fig. 2), while the maximum pressure (7.4 atm.) was measured at C34 (Fig. 2). The pressure is related to the depth of the confining layer.

The confined aquifer is characterized by regional flow of groundwater recharged as far as the heights of the Rig Anticline (Fig. 1). Recharge mechanism includes direct percolation of rainfall and snow melting. Despite the limited number of piezometers to draw a detail iso-potential map, chemical, isotopic and water temperature data and dye tracing test indicate the groundwater from the confined aquifer flows upward and also from right bank of Khersan River to left (Mohammadi et al. 2007a, b; Karimi et al. 2007). Leakage from the lower confined aquifer into the

unconfined aquifer does not occur significantly under natural conditions due to dense marly confining layer; but it locally occurs artificially, because of leakage through improperly sealed piezometers.

Hydrogeological characteristics of the confined aquifer include the following: (1) an absence of solution cavities and major conduits at outcrops and in the boreholes, (2) a low range of variation of water temperature (13.9 ± 0.77°C) and EC (381 ± 12 μS/cm) during the study period (Karimi et al. 2007), (3) a low tritium content (1.7 TU) indicating a high proportion of an old recharge (Mohammadi 2006), and (4) water velocity lower than 3 m per hour according to dye tracing test (Mohammadi et al. 2007b). Even though above characteristics were interpreted as indications of diffuse flow condition in the confined aquifer, reliable judgment needs further researches. Experience is replete with cases of the drilling wells that just missed a major cave or conduit (e.g. Merritt 1995; Worthington et al. 2000; Milanovic 2004; Mohammadi and Raeisi 2007; Perrin and Luetscher 2008 and so on). Accordingly, low variation of physico-chemical parameters and slow water velocity obtained from dye tracing test in piezometers may be simply caused by mixing of waters
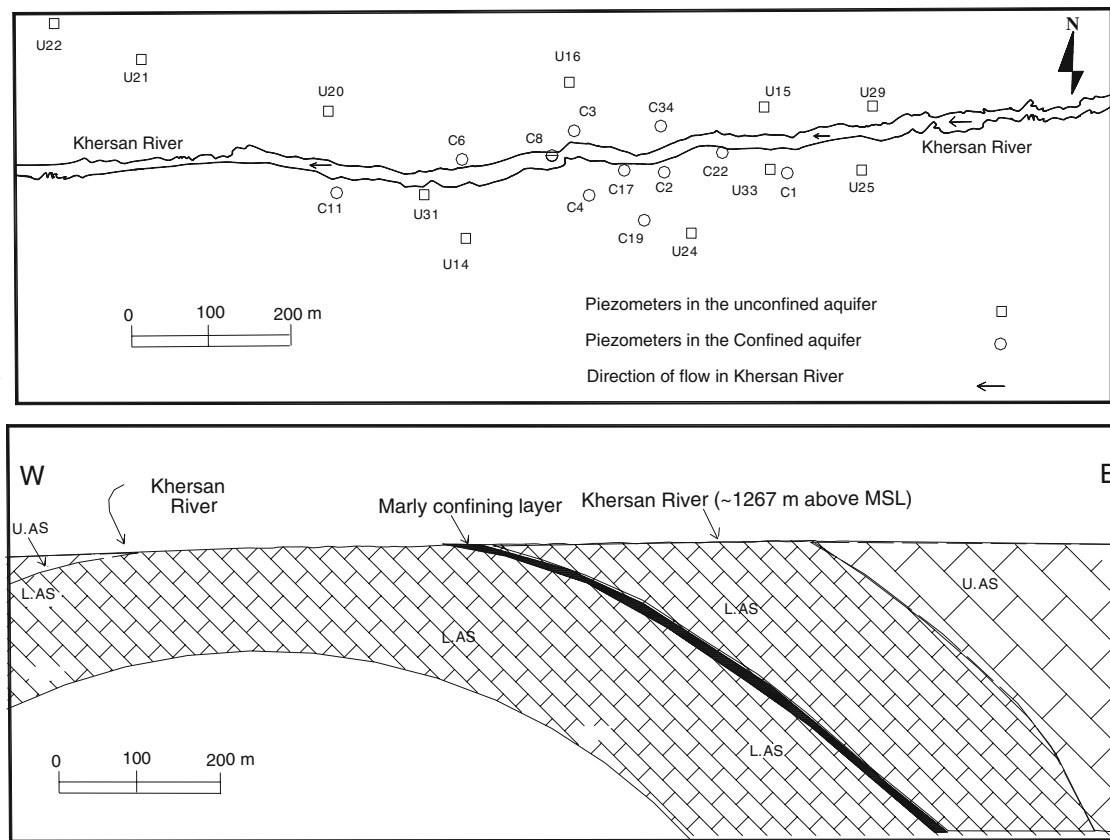

Fig. 2 Location of the unconfined (with prefix notation of *U*) and confined piezometers (with prefix notation of *C*) and a cross section of the marly confining layer, unconfined and confined aquifers along the

Khersan River (U.AS and L.AS refer to the upper and lower Asmari limestone, respectively)

moving at different velocities and pathways of different lengths and they do not exactly mean diffuse flow.

Methods

Sampling and measurements

To obtain a spatial and temporal distribution of water chemistry in the confined and unconfined aquifers, 22 piezometers and Khersan River (Fig. 2) were sampled. Samples from Khersan River, C17, C19, C34, U16, U25, U29, U31 and U33 were collected in June 2001, October 2001, January 2002 and May 2002. The other piezometers were sampled once or twice during the study period.

Temperature, pH and EC were measured in the field using ELE portable instruments. In the laboratory, the major chemical components were analyzed by the following methods: Ca^{2+}, Mg^{2+} by standard titration; Na^+, K^+ by flame photometry; Cl^- by Mohr method; HCO_3^- by titration with HCl against methyl orange indicator and SO_4^{2-} by turbidity method. The accuracy of chemical analyses was estimated from the ionic balance, showing that errors are less than 5% in all samples. PHREEQC Code (Parkhurst and Appelo 1999) was applied to calculate the saturation index with respect to calcite (SIC), dolomite (SID), gypsum (SIG) and the partial pressure of CO_2 (p_{CO_2}).

Samples from Khersan River, C17, C19, C34, U16, U25, U29, U31 and U33 were collected for isotope analysis in the beginning of dry (June 2001) and wet (January 2002) seasons. Isotope analyses were performed by the Centre for Isotopes, University of Groningen, The Netherlands. The $\delta^{18}O$ was determined based on the equilibrium of CO_2–H_2O at 25°C. The δ^2H measurements were made by the uranium reduction method. Tritium content was measured by sample enrichment to ethane and then proportional gas counting. The $\delta^{18}O$ and δ^2H contents are reported in ‰ versus standard mean oceanic water (SMOW) with a precision of about ±0.1 and ±2‰, respectively. Tritium values are reported in tritium unit (TU), with an uncertainty of ±0.2.

Principal component analysis (PCA)

PCA is a multivariate statistical technique used for data reduction and for deciphering patterns within large set of variables (Stetzenbach et al. 2001). The eigenvectors of a correlation matrix of the variable provide significant insight into the structure of the data matrix (Davis 2002). PCA would allow finding out associations between variables, thus reducing the dimensionality of the data table. This is realised by the diagonalization of the correlation matrix, which transforms the original variables into uncorrelated (orthogonal) ones (weighted linear combination of the original variables) called principal components

Table 1 Comparison between characteristics of the unconfined and confined sub-aquifers

| Parameter | The unconfined aquifer | | | | | The confined aquifer | | | | |
	N	Ave	SD	Max	Min	N	Ave	SD	Max	Min
T (°C)	32	16.73	1.71	20.70	14.20	25	14.91	1.27	17.80	13.50
EC (µS/cm)	32	456.81	38.34	560.00	387.00	25	384.64	70.24	495.00	222.00
pH	32	7.78	0.27	8.20	7.19	25	8.32	0.52	9.26	7.68
HCO_3 (mg/l)	32	231.42	27.54	298.90	176.90	25	170.07	52.10	231.80	48.80
Cl (mg/l)	32	28.21	8.02	53.10	14.16	25	23.58	6.31	35.40	7.08
SO_4 (mg/l)	32	46.72	21.34	100.11	18.80	25	65.18	30.93	187.06	38.54
Mg (mg/l)	32	28.17	4.63	36.45	18.23	25	27.29	4.71	38.88	18.23
Ca (mg/l)	32	60.62	10.13	94.19	40.08	25	48.50	12.37	70.14	18.04
Na + K (mg/l)	32	16.80	6.72	31.62	6.82	25	10.94	7.73	28.52	3.10
TDS (mg/l)	32	411.94	33.30	487.89	312.63	25	345.55	63.27	480.89	197.98
SIC	32	0.354	0.283	0.86	−0.23	25	0.6024	0.372	1.36	−0.08
SID	32	0.0265	0.548	0.87	−1.2	25	0.5812	0.753	2.02	−0.58
SIG	32	−1.927	0.215	−1.49	−2.43	25	−1.869	0.196	−1.25	−2.2
p_{CO_2}	32	4.2E-3	3.5E-3	1.5E-2	1.3E-3	25	1.3E-3	1.1E-3	3.4E-3	3.0E-5
$\delta^{18}O$‰	9	−5.56	0.28	−4.97	−5.94	13	−6.68	0.13	−6.34	−6.81
δ^2H‰	9	−28.49	4.49	−22.50	−35.80	13	−33.98	1.69	−32.00	−36.90
^3H (TU)	9	3.80	0.41	4.30	3.32	13	1.71	1.18	4.60	0.50

N number of data, Ave average value, SD standard deviation, Max maximum value, Min minimum value

as PCs (Helena et al. 2000). PCA was performed on the physical, chemical, isotope and calculated data in both aquifers using XLSTAT 4.3 (Fahmy 1999). In this study, PCA was applied to delineate the processes responsible for the chemical composition of groundwater, and its changes from dry to wet period.

Results and discussion

Hydrochemical features

Table 1 summarizes the data from both aquifers considered in that analysis. In general, the unconfined aquifer presents higher EC, water temperature, isotope composition and tritium content than in the confined aquifer. Most of samples were oversaturated with respect to calcite, which suggests a potential for precipitation of calcite. However, all samples are permanently undersaturated with respect to gypsum.

The Piper diagram of Fig. 3, which plots the proportion in meq/l of the major cations and anions, shows the main hydrochemical feature. In general, the Ca–Mg–HCO₃ facies predominate in the samples. However, the confined

aquifer shows a tendency towards Ca–Mg–HCO₃–SO₄ water type. This could be attributed to lithological effect at different aquifers.

Box plot of the chemical concentrations in the confined aquifer shows that bicarbonate has the largest dispersions (Fig. 4). The wide range of values in the bicarbonate content, from 50 to 230 mg/l, might be the result of the closed system condition with respect to atmospheric CO_2 in the confined aquifer. Wide range of bicarbonate concentration in the confined aquifer has been subjected to (1) mixing of meteoric and more closed system water, (2) different flow condition in terms of water velocity and development of karst conduit between the recharge area and sampling piezometer, and/ or (3) improperly sealing condition at some of the confined piezometers and degassing in time interval between sampling and analysis.

According to box plot of the chemical concentrations in the unconfined aquifer (Fig. 5), the sulphate content shows a significant difference between the median and maximum values and median value is almost one-third of the maximum value, suggesting local contamination input to the unconfined aquifer system. Sulphate can be provided by the outcrops of GS in the study area.

Fig. 3 Piper diagram of the both unconfined (*solid circles*) and confined (*open circles*) aquifers
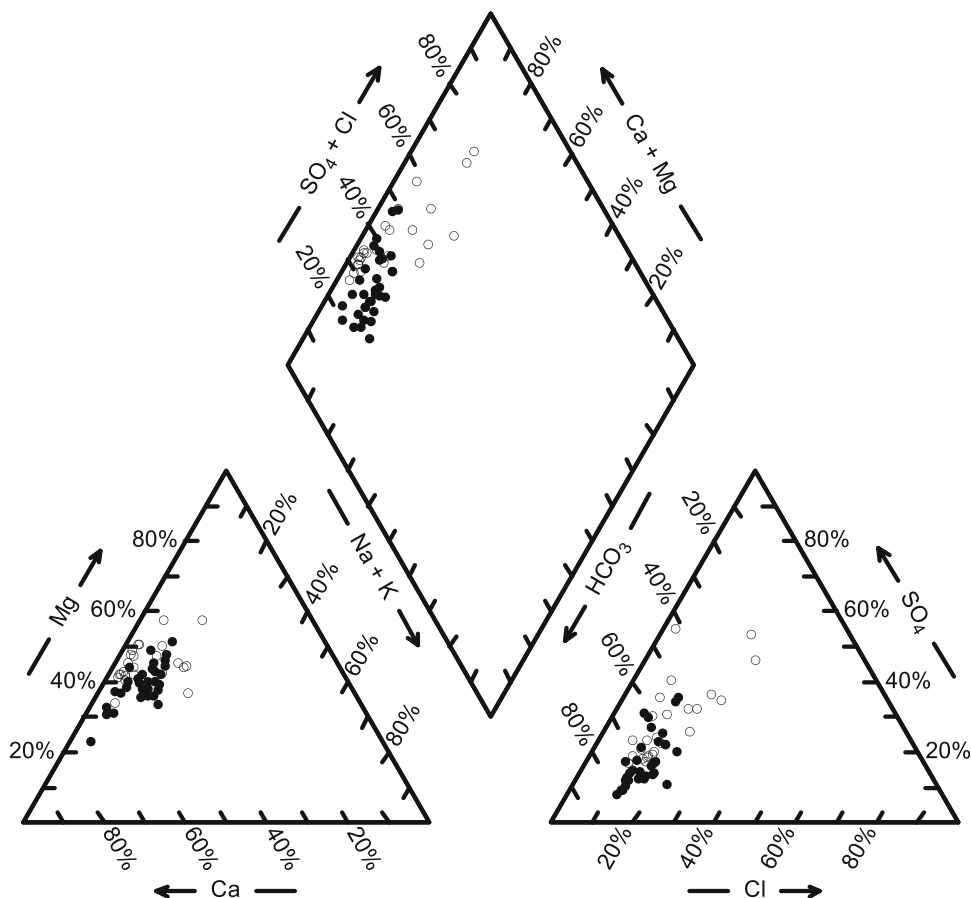
Isotope characteristics

A plot of δ^2H against $\delta^{18}O$ shows that the isotope composition of samples in the study area clusters in two groups subjected to the unconfined and confined aquifers (Fig. 6). A linear regression performed on stable isotope composition of precipitation provides the following result as local meteoric water line (LMWL) (Mohammadi 2006):

$$\delta^2H = 8.1\delta^{18}O + 20.4. \qquad (1)$$

Figure 6 shows that groundwater from the unconfined aquifer is isotopically enriched as compared to that of the confined aquifer. Oxygen-18 and deuterium contents range, respectively, from −4.97 to −5.94‰ and −22.50 to −35.80‰, in the unconfined aquifer; respectively, from −6.34 to −6.81‰ and −32.00 to −36.90‰ in the confined aquifer. This fact reflects the lower mean altitude of recharge area for the unconfined aquifer as compared to the confined aquifer.

The average tritium contents in the confined and unconfined aquifers are, respectively, 1.7 and 3.8 TU. The tritium contents in the unconfined aquifer are higher than in confined aquifer in both dry and wet seasons (Table 1) indicating a more recent recharge of the unconfined aquifer than of the confined aquifers.

Hydrochemical evolution

Several PCAs were carried out in order to screen all samples and variables. The final goal is to extract the maximum hydrogeological information from the complex data set (Bakalowicz 1994).

PCA on the whole data set

The first PCA considers 28 samples and 13 variables including T, HCO_3, Na+K, Cl, EC, Ca, SIC, SID, SO_4/TDS, Mg/TDS, Mg, SO_4 and p_{CO_2} (Table 2). The three principal axes of PCA explain about 79% of the total variance (Table 2). The maximum contribution reached by each variable is highlighted in Table 2. Principal component 1 (PC1) accounts for 42% of the total variance and appears to characterize the water–rock interaction processes resulting to water mineralization (Fig. 7a). Dissolution of the carbonate aquifer matrix includes high loadings in EC, Ca, and HCO_3. The lack of correlation between Mg–SO_4 and HCO_3 suggests both a different lithological origin (dissolution of gypsum for SO_4 and limestone-dolomite for HCO_3). PC2 represents 23.2% of the total variance and is subjected to high loading in SIC and SID opposite to p_{CO_2} (Fig. 7a). PC2 refers to important role of carbonate equilibrium in water chemistry. PC3 is dominated by loading in Mg and partly Na+K, Cl and SO_4
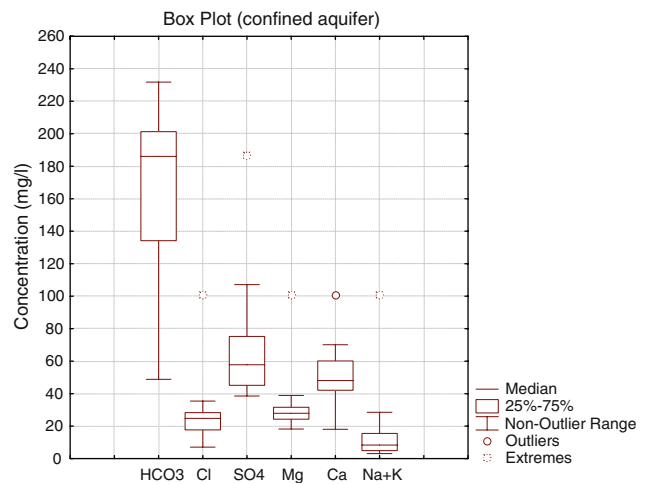

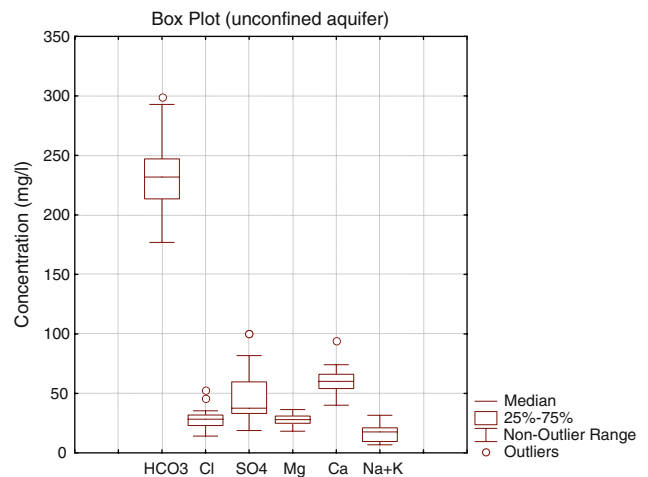**Fig. 4** Box plot of chemical composition in the confined aquifer

Fig. 5 Box plot of chemical composition in the unconfined aquifer
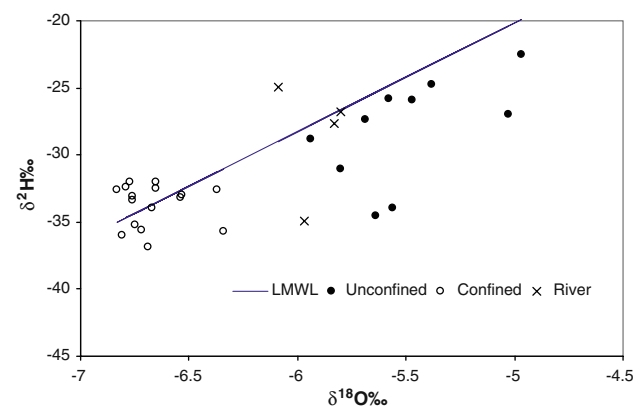

Fig. 6 Isotope composition of Khersan River and the both confined and unconfined aquifers (modified from Mohammadi 2006)

and accounts for 13.7% of the total variance. It most likely reveals the dissolution of evaporate minerals and its contribution to chemical composition.

Table 2 Factor loadings of variables on PCs in the first PCA

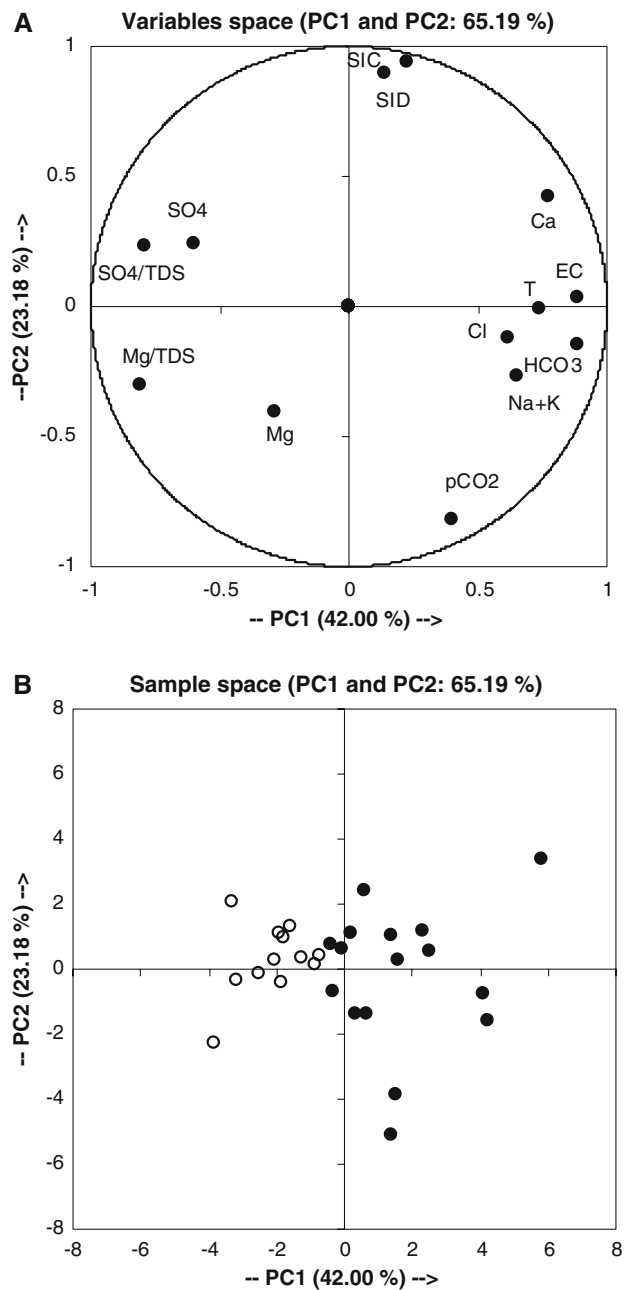| Variable	PC1	PC2	PC3
T	**0.739**	−0.013	0.173
EC	**0.883**	0.034	0.203
HCO_3	**0.888**	−0.148	0.085
Cl	**0.614**	−0.118	**0.432**
Na+K	**0.653**	−0.270	**0.588**
SIC	0.224	**0.939**	0.142
SID	0.139	**0.896**	0.270
Mg	−0.283	−0.404	**0.756**
P_{CO_2}	0.404	**−0.821**	−0.069
Ca	**0.775**	0.420	−0.031
SO_4	**−0.596**	0.245	**0.533**
Mg/TDS	**−0.807**	−0.305	0.327
SO_4/TDS	**−0.790**	0.231	0.321
Total variance (%)	42.0	23.2	13.7

Fig. 7 First PCA on hydrochemical data from the both unconfined (*solid circles*) and confined (*open circles*) aquifers. **a** Variable space, **b** sample space

In sample space (Fig. 7b), samples are grouped in two clusters which correspond to the different aquifers. Calcite dissolution under open system with respect to atmospheric CO_2 occurs in the unconfined aquifer as the main water–rock interaction processes. The confined samples plot close to negative part of PC1 and show high loading in SO_4 which may be resulted by gypsum dissolution under closed condition with respect to atmospheric CO_2. It seems that the increasing Ca concentration due to gypsum dissolution causes calcite to precipitate due to common ion effect; consequently, SO_4 contributes most to chemical composition. In addition, the CO_3 concentration decreases as calcite precipitates and this provokes the dissolution of dolomite and an increase of the Mg concentration, known as dedolomitization (Plummer et al. 1990; Lopez-Chicano et al. 2001; Appelo and Postma 2005).

PCA on selected piezometers for the beginning of dry and wet seasons

In order to access hydrochemical evolution from dry (June 2001 that indexed by d) to wet season (January 2002 that indexed by w), second PCA was applied to the selected samples from Khersan River and piezometers open to the unconfined (U16, U25, U31, U29 and U33) or the confined aquifer (C17, C19 and C34). The variables include EC, T, HCO_3, SO_4, [18]O and [3]H. The contribution of PC1 and PC2 in total variance is 52 and 24%, respectively. PC1 in positive direction shows low recharge elevation that is characterized by higher water temperature and $\delta^{18}O$ content. PC2 represents the residence time by high loading on the ^{3}H content and partly $\delta^{18}O$ (Fig. 8a).

In the sample space, two aquifers show different evolution from dry to wet season (Fig. 8b). The unconfined

samples are marked by considerable reduction in water mineralization (i.e. EC) from dry to wet period. This evolution is accompanied by decrease in water temperature and increase in sulphate concentration and tritium content, suggesting atmospheric modern water dissolve gypsum prior to recharging to the unconfined aquifer. The partly outcrop of GS over the unconfined aquifer helps gypsum to dissolve. Therefore, the mineralization in the unconfined aquifer decreases from the dry to wet season, but the
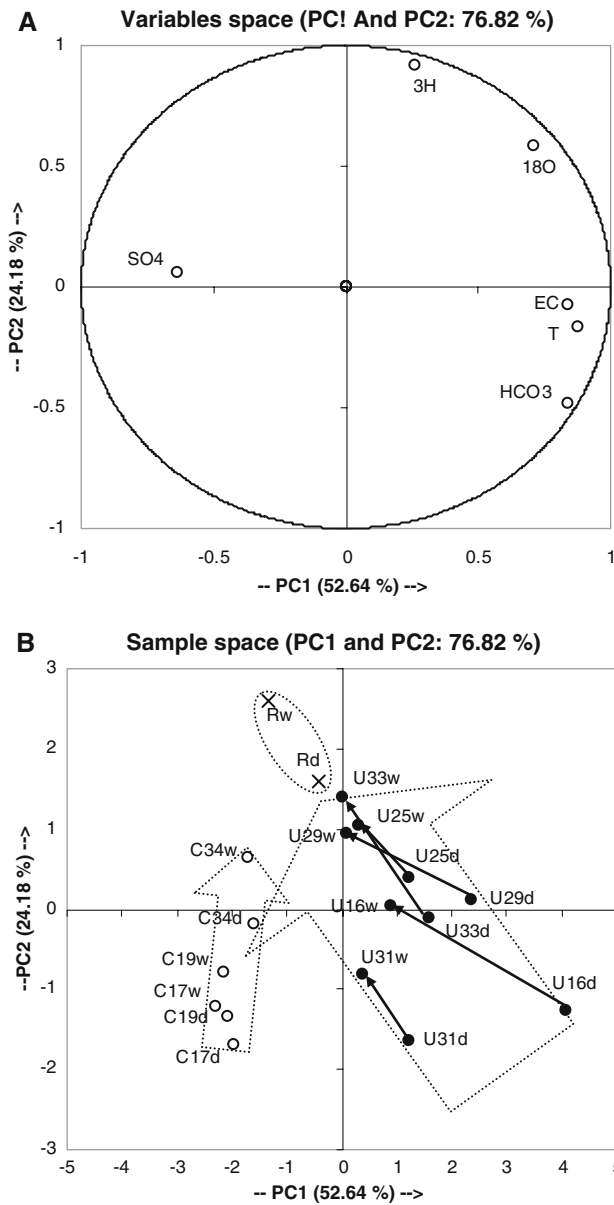
A

Variables space (PC! And PC2: 76.82 %)

B

Sample space (PC1 and PC2: 76.82 %)

Fig. 8 Second PCA on chemical and isotope data for the beginning of dry and wet seasons (denoted by *d* and *w*, respectively) in Khersan River and the both unconfined and confined aquifers (denoted by *R*, *U* and *C*, respectively). *Arrows* show trend of sample displacement from dry to wet season towards river samples

Fig. 9 Sample space of third PCA on the data obtained from the end of both wet (*open symbols*) and dry (*solid symbols*) seasons. *Circles* and *squares* show the confined and unconfined samples, respectively. Dispersion of samples at end of wet period presented by hatched area among each aquifer

river chemical composition. Therefore, there is no recharge from river to the confined aquifer.

PCA on selected piezometers for the end of dry and wet seasons

Third PCA is performed on the samples collected on both the end of dry (October 2001) and wet periods (May 2002). The used variables include Cl, *T*, EC, Ca/Mg, Ca/TDS, SO_4/TDS and SIG. The three PCs include 80% of the total variance. PCs can be interpreted same as previous PCAs. However, sample space gives more insight into the raw data. In the sample space, the unconfined samples are arranged close to each other at the end of dry period and dispersed over a large area at the end of wet period (Fig. 9). Different chemical composition of the unconfined samples at the end of recharge period was caused by (1) rising up the water table and contribution of vadose zone to chemical composition and (2) effect of surface runoff that flows over the different lithological outcrops and recharge into the unconfined aquifer. It seems that chemical composition of water in the unconfined aquifer in wet period is controlled by external processes such as recharge components and behaviour of vadose zone, but in the dry period, internal processes such as water–rock interaction in the saturated zone play as a main role. In contrast, behaviour of the confined aquifer is in different way. Meteoric water recharges to the confined aquifer over a certain area as recharge zone; consequently, chemical composition of water samples show uniformity during recharge period. Dispersion of the confined aquifer samples over a large area, shown in Fig. 8, during dry period was caused by effect of water–rock interaction and flow condition between recharge zone and sampling piezometers, i.e. flow path and velocity, which is processed under closed condition with respect to atmospheric CO_2.

contribution of gypsum layers is dominant during wet season as sulphate concentration increases. The evolution trend in the unconfined samples is toward the river sample which suggests the unconfined aquifer is recharged by the surface water. Unequal amount of displacement of the samples from dry to wet season might be subjected to karst development around to sampling piezometer. It seems that existence of a karst conduit close to U16 piezometer allows much recharge and consequently much displacement than others. The confined samples show a small displacement from dry to wet season without visible tendency toward
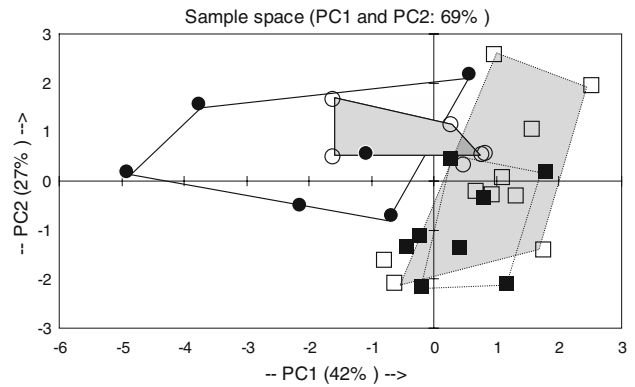
Conclusions

PCA is found to be suitable for the analysis of hydrochemical data in karst terrain. It can be seen that PCA provides more insight into karst aquifers, particularly chemical evolution from dry to wet seasons. Findings reveal that using of ions ratio in addition to the original data helps to better performance of PCA. Four sets of samples were made in order to evaluate the hydrochemical feature and evolution of the groundwater chemistry by seasonality in different flow system context (e.g. confined and unconfined aquifers).

The first PCA indicates (1) the most common chemical reaction along the flow paths is calcite dissolution and partly dolomite dissolution. Nevertheless, GS and the lithology of the lower Asmari limestone favours the occurrence of evaporate minerals such as halite and gypsum, and (2) the general occurrence of gypsum dissolution causes calcite precipitation under different p_{CO_2} condition between the confined and unconfined aquifers. Accordingly, Ca–HCO$_3$ water type in the confined aquifer changed to Ca–HCO$_3$–SO$_4$ water type due to gypsum dissolution under closed condition with respect to CO$_2$.

The second PCA shows a sharp trend, evidenced by displacement of the unconfined samples towards river samples from dry to recharge period. This trend is characterized by reducing in EC (i.e. water mineralization) and increasing contribution of the recent precipitation (i.e. tritium content). The amount of displacement of samples along this trend might be attributed to degree of karst development close to sampling site.

The third PCA reveals that in contrast to the confined aquifer, chemical composition of water samples in the unconfined aquifer tends to differ considerably from each other in the end of recharge period due to mechanism of recharge.

Despite the extensive finding in this research, additional hydrochemical and isotopic data, particularly daily time series are required to comprehensively identify the dynamics of groundwater flow and consequently chemical evolution in the study area.

References

Alavi M (2004) Regional stratigraphy of the Zagros fold-thrust belt of Iran and its proforeland evaluation. Am J Sci 304:1–20

Andreo B, Carrasco F, Bakalowicz M, Kudry J, Vadillo I (2002) Use of hydrodynamic and hydrochemistry to characterise carbonate aquifer: case study of the Blanca-Mijas unit (Malaga, southern Spain). Environ Geol 43:108–119

Appelo C, Postma D (2005) Geochemistry, groundwater and pollution. Balkema, Rotterdam, p 649

Bakalowicz M (1994) Water geochemistry: water quality and dynamics. In: Stanford J, Gilbert J, Danielopol D (eds) Groundwater ecology. Academic Press, New York, pp 97–127

Bakalowicz M (2005) Karst groundwater: a challenge for new resources. Hydrogeol J 13:148–160

Davis JC (2002) Statistics and data analysis in geology, 3rd edn. Wiley, New York, p 638

Mahab Ghods Consulting Engineers (2000) Engineering geology report on Khersan 3 Dam (unpublished)

Fahmy T (1999) XLSTAT-pro version DOIT, 6 rue de Varize, 75016 Paris, France (http://www.xlstat.com)

Ford DC, Williams PW (1989) Karst geomorphology and hydrology. Unwin Hyman, London, p 601

Glynn PD, Plummer LN (2005) Geochemistry and the understanding of groundwater system. Hydrogeol J 13:263–287

Guler C, Thyne GD, McCray JE, Turner K (2002) Evaluation of graphical and multivariate statistical methods for classification of water chemistry data. Hydrogeol J 10:455–474

Helena B, Pardo R, Vega M, Barrado E, Fernandez JM, Fernandez L (2000) Temporal evolution of groundwater composition in an alluvial aquifer (Pisuerga River, Spain) by principal component analysis. Water Res 34(3):807–816

Karimi H (2003) Hydrogeological study of aquifers in Kersan 3 Dam area using time variations of physico-chemical parameters. M.Sc. Thesis, Department of Earth Sciences, Shiraz University, Shiraz, Iran (unpublished)

Karimi H, Raeisi E, Bakalowicz M (2005) Characterising the main karst aquifers of the Alvand basin, northwest of Zagros, Iran, by a hydrogeochemical approach. Hydrogeol J 13:787–799

Karimi H, Keshavarz T, Mohammadi Z, Raeisi E (2007) Potential leakage at the Khersan 3 Dam site, Iran: a hydrogeological approach. Bull Eng Geol Environ 66:269–278

Lopez-Chicano M, Bouamama M, Vallejos A, Pulido-Bosch A (2001) Factors which determine the hydrogeochemical behaviour of karstic springs. A case study from the Betic Cordilleras, Spain. Appl Geochem 16:1179–1192

Merritt AH (1995) Geotechnical aspects of the design and construction of dams and pressure tunnel in soluble rocks. In: Beck BF (ed) Karst geohazards: engineering and environmental problems in karst terrane. AA Balkema, Rotterdam, pp 3–7

Milanovic PT (2004) Water resources engineering in karst. CRC Press, Boca Raton, p 312

Mohammadi Z (2006) Method of leakage study at karst dam site, the Zagros region. Ph.D. dissertation, Department of Earth Science, Shiraz University

Mohammadi Z, Raeisi E (2007) Hydrogeological uncertainties in delineation of leakage at karst dam sites, the Zagros Region, Iran. J Cave Karst Stud 69(3):305–317

Mohammadi Z, Raeisi E, Bakalowicz M (2007a) Evidence of karst from behavior of the Asmari limestone aquifer at the Khersan3 dam site, Southern Iran. Hydrol Sci J 52(1):206–220

Mohammadi Z, Raeisi E, Zare M (2007b) A dye tracing test as an aid of karst development study at the artesian limestone sub-aquifer: Zagros Zone, Iran. Environ Geol 52:587–594

Parkhurst DL, Appelo CAJ (1999) User's guide to PHREEQC (version 2) a computer program for speciation, batch-reaction, one-dimensional transport and inverse geochemical calculations. US Geological survey, Water resources investigation report 99–4259, pp 312

Perrin J, Luetscher M (2008) Inference of the structure of karst conduits using quantitative tracer tests and geological information: example of the Swiss Jura. Environ Geol 16:951–967

Plummer LN, Busby JF, Lee RW, Hanshaw BB (1990) Geochemical modeling of the Madison aquifer in parts of Montana, Wyoming, and South Dakota. Water Resour Res 26(9):1981–2014

Raeisi E, Kowsar N (1997) Development of Shahpour Cave, southern Iran. J Cave Karst Sci 24(1):27–34

Stetzenbach KJ, Hodge VF, Guo C, Farnham IM, Johannesson KH (2001) Geochemical and statistical evidence of deep carbonate groundwater within overlying volcanic rock aquifers/aquitards of southern Nevada, USA. J Hydrol 243:254–271

Stocklin J (1968) Structural history and tectonics map of Iran: a review. Am Assoc Pet Geol Bull 52(7):1229–1258

Stocklin J, Setudehnia A (1977) Stratigraphic lexicon of Iran. Geological survey of Iran, pp 376

Worthington SRH, Ford DC, Beddows PA (2000) Porosity and permeability enhancement in unconfined carbonate aquifers as a result of solution. In: Klimchouk A, Ford DC, Palmer AN, Dreybrodt W (eds) Speleogenesis: evolution of karst aquifers. National Speleological Society, Huntsville, pp 463–472